Isolation and Characterization of Vitreous Insulin-like Growth Factor Binding Proteins

Clyde Guidry and Jeffery L. King

Purpose. Previous studies from this laboratory revealed that vitreous insulin-like growth factor (IGF) biological activity increases in proliferative diabetic retinopathy and that this activity is normally attenuated by IGFBPs. The goal of this study was to identify and characterize the species involved.

Methods. Human and porcine vitreous, plasma, recombinant IGFBP-2, and IGFBP-3 were separated by gel electrophoresis. Functional IGFBPs were detected in Western ligand blots with biotinylated IGF-II. IGFBPs were identified using IGFBP-specific antibodies.

Results. Western ligand blots of normal vitreous and plasma detected two major proteins at ~35 kDa and ~29 kDa. Western blot analysis of human and porcine vitreous and plasma confirmed the identity of the ~35-kDa band as IGFBP-2 and the ~29-kDa band as a fragment of IGFBP-3. Western blot and Western ligand blot analyses of vitreous and plasma proteins separated by two-dimensional gel electrophoresis revealed that the IGFBP-3 fragments in vitreous and plasma have virtually identical profiles. Lyase digestion revealed that the ~29-kDa IGFBP-3 fragment is a glycoprotein with a peptide core of ~25 kDa. N-terminal sequence data obtained from vitreous IGFBP-3 revealed that the protein is proteolytically truncated at the C terminus.

Conclusions. Normal human and porcine vitreous contain two major IGFBPs, IGFBP-2 and an ~29-kDa fragment of IGFBP-3. Both IGFBPs retain biological activity, and IGFBP-3 has one or more glycosylation sites with a protein core of ~25 kDa. Systematic comparisons indicate that the vitreous IGFBP-3 is similar to and perhaps identical with a previously described IGFBP-3 fragment in plasma with reduced growth factor affinities. (*Invest Ophthalmol Vis Sci.* 2011;52:303–309) DOI: 10.1167/iovs.10-5920

Proliferative diabetic retinopathy (PDR) is a late-stage complication of diabetes in which fibrovascular tissues emerge from the retina and exert tractional forces that can cause retinal detachment.[1] Though complex and incompletely understood, PDR is ultimately a cellular disorder involving a progression of specific activities that minimally include cell translocation from the retina, cell division, and the generation of tractional forces.[2]

There is considerable interest in identifying the causal cell types and the stimuli leading to their pathogenic activities because the ability to arrest or attenuate any of these processes would represent a significant gain in control of this complication. Immunohistochemical studies of diabetic epiretinal tissues have identified a number of different cell types, including glia, immune cells, retinal pigment epithelial cells, and fibroblastlike cells of unknown origin.[3–8] Müller cells, the principal retinal glia, are consistently identified in diabetic fibrovascular scar tissues using the traditional immunocytochemical markers glial fibrillary acidic protein and glutamine synthetase.[3,6,8,9] In addition, more recent studies from this laboratory revealed that the fibroblastlike cells mentioned are also derived, at least in part, from phenotypically altered Müller cells.[9] Described was a progressive loss of glial-specific proteins and de novo expression of alpha smooth muscle actin ending with myofibroblast-like cell types that are unrecognizable as glia in a process that closely resembles phenotype changes previously described in primary cultures of Müller cells.[10,11]

There is also abundant circumstantial evidence indicating that Müller cells are a source of the tractional forces that cause retinal detachment in PDR. Although freshly isolated, phenotypically recognizable Müller cells lack the capacity to generate tractional forces, this is not the case with the fibroblastlike phenotype described.[11,12] In concert with a phenotype change, and in particular with de novo expression of α-smooth muscle actin, Müller cells acquire the capacity for tractional force generation in culture. Systematic study of Müller cell tractional force generation in vitro revealed that this activity is not constitutive but is instead stimulated by certain exogenous promoters, including ligands, in the insulin-like growth factor and platelet-derived growth factor systems.[11,12] Consistent with these findings, tractional force–stimulating activity to which Müller cells respond is present in diabetic, but not in normal, vitreous, and studies with growth factor–neutralizing antibodies attributed most of this activity to IGF-related ligands.[13]

As a consequence of these findings, there is now considerable interest in gaining an improved understanding of vitreous changes in diabetes and, in particular, those that result in increased IGF biological activity. Several laboratories have examined diabetes-associated changes in vitreous IGF-I and IGF-II levels, reporting increases varying between 150% and 300%.[14–20] However, the values reported for normal vitreous correlate poorly with the observed absence of biological activity, leading us to speculate that a control mechanism attenuates vitreous ligands.[13,21] The insulin-like growth factor system also contains six high-affinity insulin-like growth factor binding proteins (IGFBPs) that can potentiate or inhibit IGF activities and can also have direct growth factor–independent effects.[22–27] Several laboratories used ELISA-type assays to examine IGFBP levels in normal and diabetic vitreous and reported detecting IGFBP-2 and IGFBP-3.[15,18,20] We have since examined the effects of all six IGFBPs on Müller cells generating tractional forces in response to IGF and determined that IGFBP-2 and IGFBP-3 are potent inhibitors of IGF-I and IGF-II activities.[28]

From the Department of Ophthalmology, University of Alabama School of Medicine, Birmingham, Alabama.

Supported by National Institutes of Health Grant EY13258, EyeSight Foundation (Birmingham, Alabama), and a departmental award from Research to Prevent Blindness.

Submitted for publication May 20, 2010; revised August 5, 2010; accepted August 21, 2010.

Disclosure: **C. Guidry**, None; **J.L. King**, None

Corresponding author: Clyde Guidry, Department of Ophthalmology, University of Alabama School of Medicine, EFH DB106, Birmingham, AL 35294; cguidry@uab.edu.

Together these observations led us to propose that IGFBPs in normal vitreous function as a growth factor sink, limiting the concentration of free ligand and thus controlling IGF biological activity.[28] However, there are several confounding elements to this hypothesis, including a report suggesting that IGFBP-3 in normal vitreous is cleaved to an inactive form by local proteases.[29] In addition, IGFBP levels in vitreous reportedly increase rather than decrease in diabetes, suggesting that these changes may be pathogenic rather than protective.[15,18,20] The goal of this project was to determine which IGFBPs are present in normal vitreous and to determine which of these retain the capacity to bind IGF ligands and thus modulate growth factor biological activity.

METHODS

Vitreous

Porcine eyes were removed immediately after euthanatization and transported to the laboratory in ice-cold saline. The globes were cleaned of extraneous tissue, rinsed with ice-cold saline, and opened with a hemispheric cut using a razor blade and iris scissors. The vitreous was removed intact and stored frozen until used for experimentation. The methods used to secure animal tissue were humane and complied with the ARVO Statement for the Use of Animals in Ophthalmic and Vision Research. Human vitreous samples were removed using the same approach on donor eyes provided by the Alabama Eye and Tissue Bank (Birmingham, AL), with postmortem times ranging from 2 to 5 hours.

Western Ligand Blot Analysis

Experiments to evaluate vitreous IGFBPs were performed using our previously reported protocols.[30] Vitreous samples were combined with nonreducing Laemmli sample buffer,[31] heated to 100°C for 3 minutes, and separated at 20 mA on 10% sodium dodecyl sulfate–polyacrylamide gels. Proteins were transferred to nitrocellulose membranes (Hybond ECL; Amersham Pharmacia Biotech, Piscataway, NJ) for 2 hours at 100 V and blocked with 3% BSA in tris-buffered saline (TBS; 0.15 M NaCl, 0.02 M tris-HCl, pH 7.8) for 60 minutes at room temperature.

Proteins were separated in two-dimensional gel electrophoresis using an isoelectric focusing system (Protean IEF Cell; Bio-Rad, Hercules CA) and immobilized pH gradient strips (ReadyStrip; Bio-Rad), pH range 3 to 10, followed by vertical gel electrophoresis as described earlier. IGFBPs were detected with 20 ng/mL biotinylated IGF-II (GroPep, Ltd., Adelaide, Australia) in TBS with 0.05% Tween-20 (TBST) for 3 hours at room temperature. Bound IGF-II was detected with 10 ng/mL horseradish peroxidase-conjugated deglycosylated avidin (NeutraAvidin; Pierce, Rockford, IL) in TBST for 60 minutes at room temperature. Chemiluminescence development was according to the manufacturer's instructions (SuperSignal West Femto; Pierce) and the membranes were exposed to film (Hyperfilm; Amersham).

Western Blot Analysis

Vitreous samples were prepared and electrophoresed as described earlier. Nitrocellulose membranes containing the transferred proteins were blocked for 1 hour at room temperature with 3% nonfat dry milk in TBST. IGFBPs were detected using mouse monoclonal antibodies against IGFBP-2 (Upstate Biotechnology Inc., Lake Placid, NY) and IGFBP-3 (Diagnostic Systems Laboratories, Webster, TX) diluted in blocking solution. After a 2-hour incubation in primary antibody, blots were incubated for 1 hour with horseradish peroxidase–conjugated goat anti–mouse IgG from Jackson ImmunoResearch Inc. (West Grove, PA) diluted in blocking buffer at 1:200,000. Chemiluminescence development was as described for Western ligand blot analysis. Recombinant IGFBP 2 and IGFBP 3 were obtained from GroPep.

Vitreous IGFBP-3 Purification

Porcine vitreous (100 mL) was acidified by the addition of 5.75 mL glacial acetic acid, stirred for 30 minutes on ice, and centrifuged to remove insoluble material. Ethanol was added successively to the supernatants to achieve 40% (vol/vol) and 80% (vol/vol), after which the mixtures was stirred on ice for 60 minutes and centrifuged to collect the insoluble material. The 80% ethanol pellet was resuspended and dialyzed overnight against PBS, after which it was fractionated by affinity chromatography on a 2.0 mL column (Affi-Gel 15; Bio-Rad) derivatized with 1 mg IGF-II (Novozymes, Bagsvaerd, Denmark). Proteins bound to the column after washes with 10 column volumes of PBS were eluted with 5 mL 0.5 M acetic acid. The affinity column eluant was fractionated by reverse-phase high-pressure liquid chromatography (PRP-Infinity, Hamilton Company, Reno NV) using a water-acetonitrile gradient supplemented with 0.1% (vol/vol) trifluoroacetic acid.

Other Reagents

Glycerol-free amidase was purchased (PNGase-F; New England Biolabs, Beverly, MA).

RESULTS

Ligand and Western Blot Analyses to Detect Functional IGFBPs in Normal Vitreous

Samples of normal human vitreous were evaluated for biologically active IGFBPs in Western ligand blots probed with biotinylated IGF-II. Two bands were consistently detected with estimated relative masses of 35 kDa and 29 kDa (Fig. 1, lane 1). The same evaluation of normal human plasma detected two similarly sized proteins and two more prominent, higher mo-

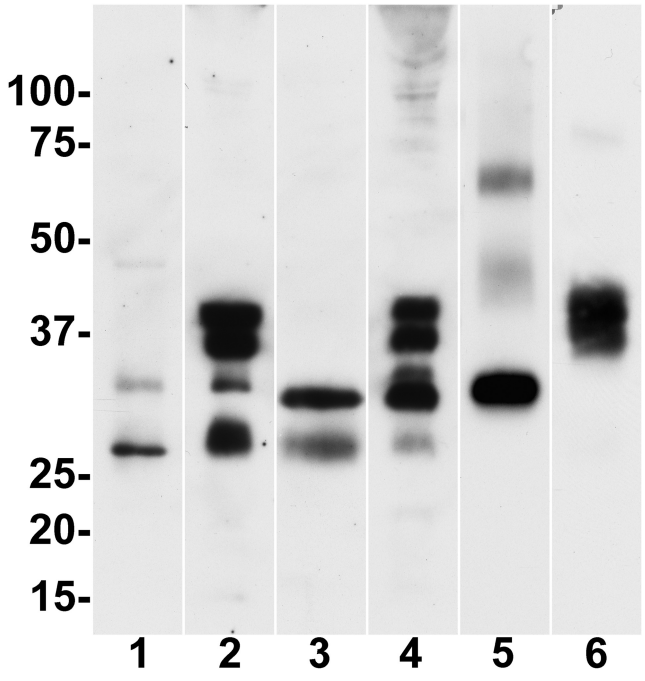

FIGURE 1. IGFBPs in vitreous and plasma detected by Western ligand blot analysis. Samples of normal human vitreous (*lane 1*) and human plasma (*lane 2*) were separated by gel electrophoresis, transferred to nitrocellulose, and probed for the presence of functional IGFBPs with biotinylated IGF-II. These results are compared with samples of normal porcine vitreous (*lane 3*), normal porcine plasma (*lane 4*), recombinant IGFBP-2 (*lane 5*) and IGFBP-3 (*lane 6*). The positions of molecular weight standards are indicated on the *left*.

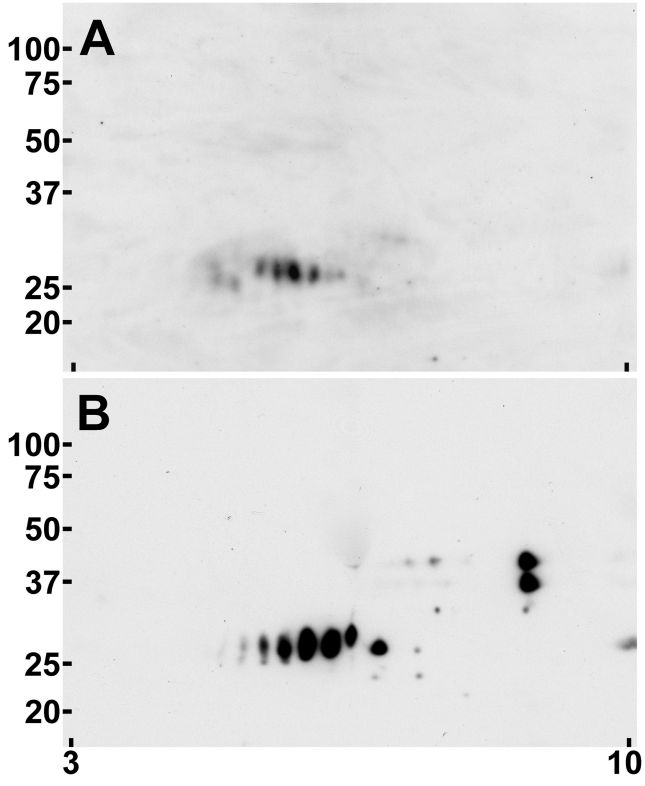

FIGURE 2. IGFBP characterization by two-dimensional Western ligand blot analysis. Samples of normal human vitreous (**A**) and normal human plasma (**B**) were separated by two-dimensional gel electrophoresis, transferred to nitrocellulose, and probed with biotinylated IGF-II. The pH range and positions of the molecular weight standards are indicated on the *bottom* and *left* of the figure, respectively.

lecular weight bands (lane 2). Comparisons with recombinant IGFBP-2 (lane 5) indicated that the 35-kDa bands in vitreous and plasma comigrate with IGFBP-2. However, this was not the case with recombinant IGFBP-3 (lane 6). Although the ~44-kDa doublet was visible in human plasma, there was no evidence of the intact IGFBP-3 in vitreous. To address concerns about postmortem proteolysis in human tissues, the same studies were performed with normal porcine vitreous harvested under carefully controlled conditions (lane 3). As with human vitreous, only two bands were detected with almost identical estimated molecular weights of 34 kDa and 29 kDa, and intact IGFBP-3 was not detected. However, like human plasma, these proteins and the same lower molecular weight bands were present in porcine plasma (lane 4).

Vitreous IGFBPs were evaluated and compared with plasma using IGF-II ligand blots of protein resolved on two-dimensional gels. In human vitreous the 29-kDa species resolved as a series of six discrete spots with estimated isoelectric points ranging from 5.38 to 6.42 (Fig. 2A) and a more basic, higher molecular weight species. Ligand blots of porcine vitreous produced the same pattern of six proteins spanning a slightly broader pH range from 4.86 to 6.48 and the higher molecular weight species (not shown). Six spots of similar molecular weight were also present in human plasma with calculated isoelectric points ranging from 5.15 to 6.53 (Fig. 2B) and several more basic, higher molecular weight species. We also performed Western immunoblot analysis on two-dimensional gel–separated proteins using monoclonal antibodies against IGFBP-2 and IGFBP-3. Anti–IGFBP-2 detected an elongated species of ~35 kDa spanning a calculated pH range from 6.74 to 7.42 in human vitreous (Fig. 3A) and human plasma (Fig. 3B). Immunoblots with anti–IGFBP-3 detected the ~29-kDa species as a row of spots within an estimated pH range of 5.35 to 6.53 and of 5.21 to 6.68, respectively (Figs. 3C, 3D).

These results led us to conclude that normal human and porcine vitreous contain two functional IGFBPs. The larger of the two measures ~35 kDa, matches intact IGFBP-2 in size, and reacts with monoclonal anti–IGFBP-2. A second lower molecular weight species of ~29 kDa reacts with monoclonal IGFBP-3 but does not resemble the intact protein in size, suggesting that it may be a fragment of the intact protein. Interestingly, we detected similarly sized anti–IGFBP-3 reactive fragments in both vitreous and plasma, suggesting that they may be of similar origins. Significantly, we detected no evidence of intact IGFBP-3 in normal vitreous of either human or porcine origin.

Characterization of Vitreous IGFBP-3

To gain more information about vitreous IGFBP-3, we considered its molecular structure. Intact IGFBP-3 reportedly contains

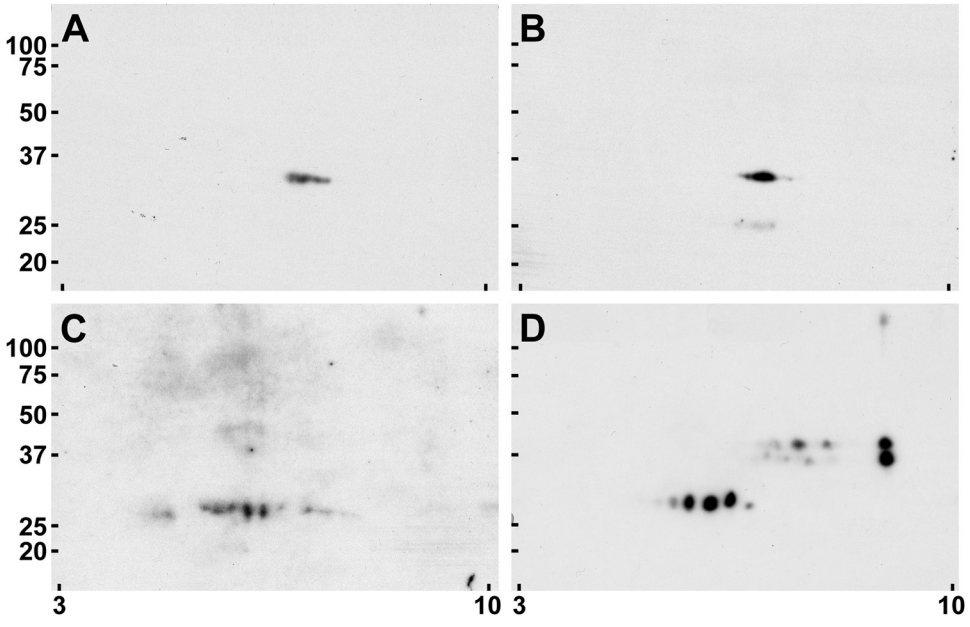

FIGURE 3. IGFBP characterization by Western blot analysis. Samples of normal human vitreous (**A**, **C**) and normal human plasma (**B**, **D**) were separated by two-dimensional gel electrophoresis, transferred to polyvinylidene difluoride, and probed with monoclonal antibodies against IGFBP-2 (**A**, **B**) and IGFBP-3 (**C**, **D**). The pH range and positions of molecular weight standards are indicated on the *bottom* and *left* of the figure, respectively.

~15 kDa N-linked sugar chains, the loss of which could theoretically account for the smaller size of the ~29-kDa fragment.[32] To test for this possibility, we examined the effects of an endoglycosidase with the ability to remove the N-linked sugars on intact and vitreous IGFBP-3. As one would predict, recombinant IGFBP-3 incubation with PNGaseF resulted in a pronounced reduction in protein size from ~44 kDa to ~33 kDa (Fig. 4A). Vitreous incubation with PNGaseF produced a similarly pronounced, approximately 9-kDa shift in the IGFBP-3 fragment and no apparent change in IGFBP-2 (Fig. 4B), indicating that only the former protein contains N-linked sugars. Control PNGaseF digests in which recombinant IGFBP-3 was combined with vitreous (Fig. 4C) produced the same protein cores as when digested separately (compare with Figs. 4A and 4B), indicating that the amount of enzyme was sufficient to produce terminal reaction products. In addition, similar incubations performed in the absence of PNGaseF produced no change, indicating that the mass reductions were attributable to the lyase and not to other contaminating proteases (Fig. 4D).

Comparisons of human plasma (Fig. 5A) and human vitreous (Fig. 5B) digested under the same conditions with PNGaseF revealed a comparable loss of mass in the ~29-kDa fragments, suggesting that they are structurally similar. This premise is further supported by ligand blots of PNGase digests of human plasma (Fig. 5C) and vitreous (Fig. 5D) subjected to two-dimensional gel electrophoresis. In this case the IGFBP-3 fragment core was resolved as a set of three uniquely positioned spots at an estimated pH range of 6.3 to 7.3. These data suggest that the smaller size of vitreous IGFBP-3 can be attributed to loss of the protein core rather than N-like sugar chains and that the putative IGFBP-3 fragments in vitreous and plasma are similar in size, isoelectric point, and N-linked sugar.

To obtain N-terminal sequence data from the vitreous IGFBP-3 fragment, we purified chemical quantities of the protein in a three-step procedure described in Methods. In preparation for affinity chromatography, vitreous was acid-dissociated with the addition of acetic acid, followed by selective precipitation with ethanol that provided nearly quantitative recovery of the protein (Fig. 6A, lane 4). After dialysis against a neutral pH buffer, vitreous IGFBP-3 was bound to an IGF-II affinity column and eluted with an acetic acid buffer (Fig. 6A, lane 7). The eluted proteins were then fractionated by reverse-phase chromatography (Fig. 6B), and the purity was evaluated by gel electrophoresis (Fig. 6C). Protein adsorbed to polyvinylidene difluoride as for Western ligand blot analysis was submitted for N-terminal sequencing, and the residues detected were the same as those at the N terminus of intact, fully processed IGFBP-3 (Table 1). Together, these data confirm that the fragment is indeed derived from IGFBP-3, and the N-terminal sequence data and deglycosylation findings indicate that the smaller size of vitreous IGFBP-3 is attributable to proteolytic cleavage at the C terminus.

Vitreous IGFBP-3 Protease

Finally, we wanted to determine whether the vitreous IGFBP-3 fragment we detected was a product of the previously described IGFBP-3–specific protease reported to be present in vitreous.[29] Consistent with the previous study, the addition of small amounts of normal human vitreous and human serum resulted in rapid cleavage of the intact protein to a smaller ~29-kDa fragment (Fig. 7A), and incubation of serum without vitreous resulted in only minor changes in fragment abundance (Fig. 7B). However, when we incubated recombinant IGFBP-3 with the same amount of vitreous, there was no evidence of protein cleavage (Fig. 4C). This result suggested that both serum and vitreous were necessary for IGFBP-3 cleavage, a premise that was confirmed in an experiment in which recombinant IGFBP-3 was incubated with vitreous and serum (Fig. 4D). Experiments of identical design using normal porcine vitreous generated the same results (not shown), indicating that the absence of IGFBP-3 proteolytic activity in normal vitreous is neither a species-related phenomenon nor related to the longer postmortem collection times associated with human vitreous samples.

Discussion

The goal of this study was to identify and characterize the IGFBPs in normal vitreous that are likely to be biologically active, defined in this case by demonstrable affinity for one or more of the IGF ligands. In this our results are relatively straightforward. Western ligand blot analysis performed with IGF-II detected two major IGFBP species that were identified in subsequent experiments as IGFBP-2 and IGFBP-3. Based on their observed affinity for IGF-II, both these vitreous binding proteins have the capacity to modulate the pool of free growth factor and thus impact net vitreous biological activity. Because there is no evidence of substantial quantities of any other similarly functional IGFBPs, it seems reasonable to conclude that IGFBP-2 and IGFBP-3 are the major binding proteins in vitreous and are the only proteins whose growth factor affinities can be considered part of the normal control mechanism of vitreous IGF biological activity.

Another potentially important observation is that IGFBP-3 in normal human and porcine vitreous exists as a biologically active fragment derived from the N terminus of intact IGFBP-3. Although the ligand blots and affinity chromatography demonstrate that this protein still has affinity for IGF ligands, how this compares with the intact protein is uncertain. We expended considerable effort comparing the physical characteristics of the vitreous and serum fragments and found them to be similar in every respect, including size, isoelectric point, and N-linked glycosylation. In light of these obvious similarities, we speculate that the two fragments have similar biological activities. Ahlsen et al.[33] compared to intact IGFBP-3 and the plasma

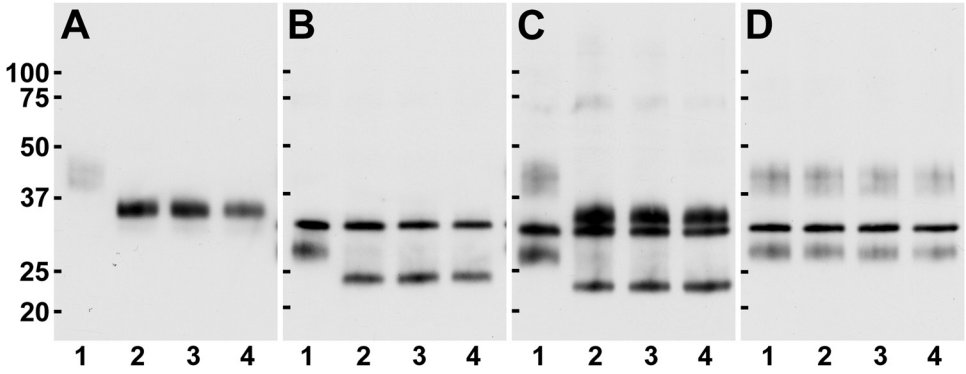

Figure 4. Molecular characterization of vitreous IGFBP glycosylation. Samples of recombinant IGFBP-3 (**A**) and normal human vitreous (**B**) were incubated with PNGaseF for 0 (*lane 1*), 0.5 (*lane 2*), 1 (*lane 3*), and 2 hours (*lane 4*) and then probed in Western ligand blots. These results were compared with control incubations containing recombinant IGFBP-3 plus vitreous with (**C**) and without (**D**) PNGase F. The positions of molecular weight standards are indicated at the *left* of the figure.

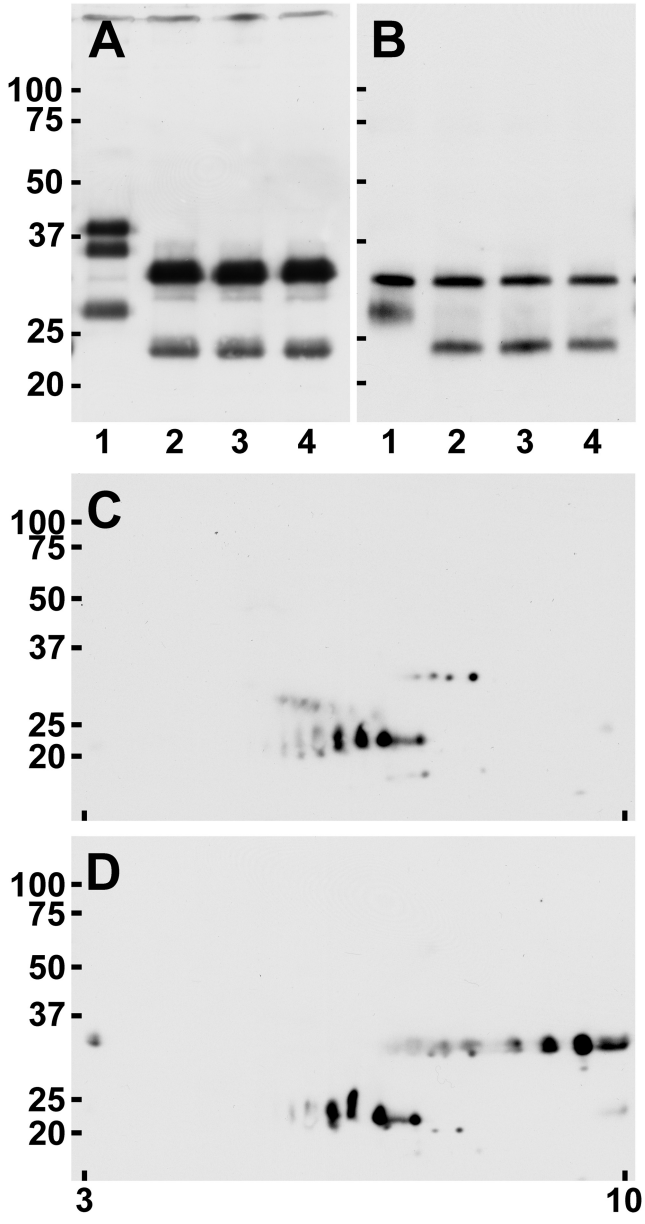

FIGURE 5. Vitreous fragment glycosylation compared with plasma. Samples of normal human plasma (**A**) and normal human vitreous (**B**) were incubated with PNGaseF for 0 (*lane 1*), 0.5 (*lane 2*), 1 (*lane 3*), and 2 (*lane 4*) hours, after which the samples were evaluated by Western ligand blot analysis. Vitreous (**C**) and plasma (**D**) samples incubated with PNGaseF for 2 hours were also separated by two-dimensional gel electrophoresis and evaluated in Western ligand blots. The pH range and positions of molecular weight standards are indicated on the *bottom* and *left* of the panels, respectively.

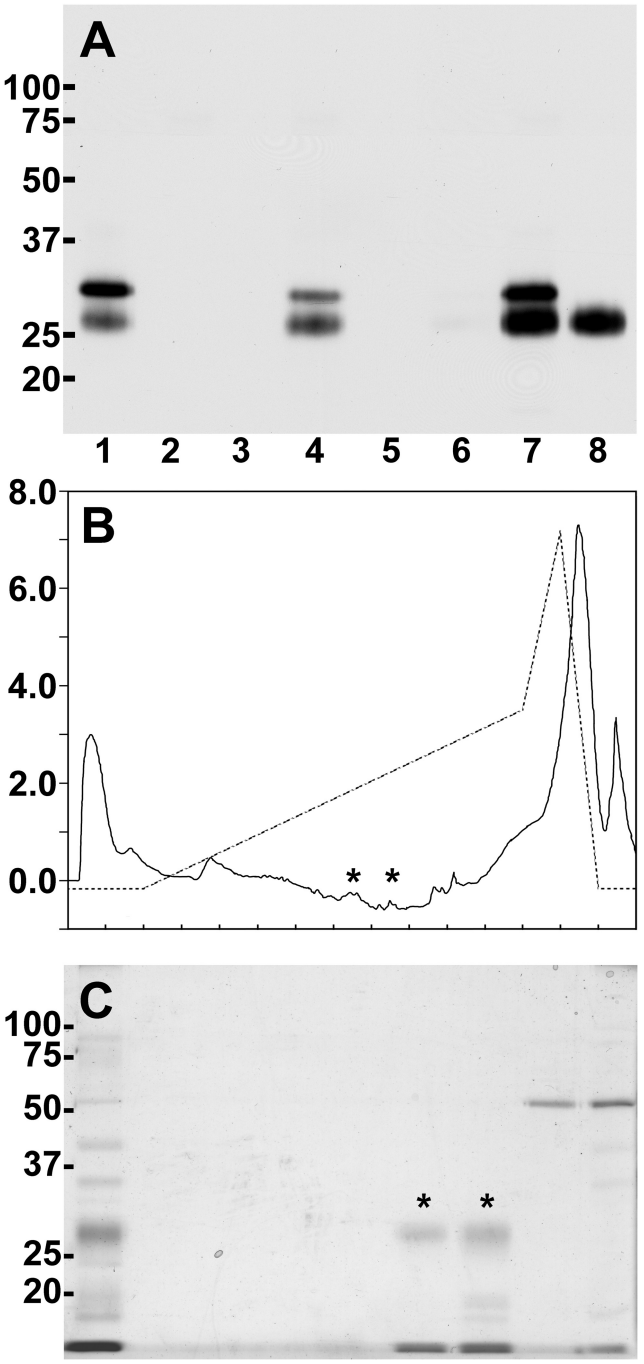

FIGURE 6. Vitreous IGFBP-3 purification. Porcine vitreous was acidified, subjected to sequential ethanol precipitation, and fractionated by IGF-II affinity chromatography. Samples from each stage of the process were analyzed by Western ligand blot analysis (**A**), including the starting material (*lane 1*), acidified vitreous pellet (*lane 2*), 40% ethanol pellet (*lane 3*), 80% ethanol pellet (*lane 4*), 80% ethanol supernatant (*lane 5*), affinity column flow-through (*lane 6*), and affinity column bound (*lane 7*). This material was then fractionated by reverse-phase chromatography using a water acetonitrile gradient (**B**). Samples from the active fractions identified by Western ligand blot analysis (not shown) were stained with Coomassie Blue (**B**), pooled, and then probed by Western ligand blot analysis (*lane 8*, **A**). The positions of molecular weight standards are indicated at the *left* of **A** and **C**. Protein milli-absorbance units at 280 nm are indicated (**B**).

fragment's affinities for IGF-I and IGF-II and reported decreases of 11-fold and 4-fold, respectively, that were largely attributed to an increased off rate. Along this same line, Yan et al.[34] demonstrated that the plasma IGFBP-3 fragment retains the ability to assemble into the tertiary complex with a ligand and the acid-labile subunit provided that the C-terminal fragment is also available for assembly. Under these conditions, the fragment also retains the ability to inhibit IGF transport across endothelial layers and IGF ligand receptor phosphorylation. These results suggest that the net effect of the IGFBP-3 fragment is to reduce vitreous IGF biological activity. However, it

TABLE 1. Porcine IGFBP-3 Sequence Analysis

MQRARPALWA AALIALALLR GPPAARAGSG AAGTGPVVRC
EPCDARALAQ CAPPPAAPPC AELVREPGCG CCLTCALREG
QACGVYTERC GAGLRCQPPP GEPRPLQALL DGRGICANAS
AAGRLRAYLL PAPPAPGNGS ESEEDRSVDS MENQALPSTH
RVPDSKLHSV HTKMDVIKKG HAKDSQRYKV DYESQSTDTQ
NFSSESKRET EYGPC RREME DTLNHLKFLN MLSPRGIHIP
NCDKKGFYKK KQCRPSKGRK RGFCWCVDKY GQPLPGFDVK
GKGDVHCYSM ESK

Amino acids identified by N-terminal sequencing are underlined and bold. Porcine sequence data are from accession number P16611.

also seems unlikely that the IGFBP-3 fragment has the high capacity to attenuate IGF-I and IGF-II biological activity through sequestration as we reported for the intact protein.[28] On the other hand, it is possible that the IGFBP-3 fragment, like the parent molecule, has cell-direct activities that must be considered in determining this protein's role in vitreous biochemistry. To our knowledge, IGFBP-2, IGFBP-3, or the IGFBP-3 fragment's direct effects, have not been studied on any IGF-responsive ocular cells relevant to proliferative vitreoretinopathies, making this an important area for future study.

These results are consistent with many of the observations, but not necessarily the conclusions, of previously published studies in this field. Several laboratories reported vitreous levels of IGFBP-2 and IGFBP-3 in surgical samples from diabetic and nondiabetic patients using immune assays such as ELISA and RIA.[15,18,20] These assays might have been influenced by the knowledge that they were, in part, measuring an IGFBP-3 fragment rather than an intact protein. Depending on the specificity of the antibody used in these assays, the size differences in an equally reactive protein core could lead to protein concentration overestimates by as much as 35%. Alternatively, immunoreactivity involving the missing C-terminal portion of the core would have caused a gross underestimation of protein abundance. Given that we have not yet determined whether IGFBP-3 in pathologic vitreous is truncated to the same degree as normal vitreous, the influence of these findings are still uncertain. One study of direct relevance examined vitreous binding protein abundance in cadaveric controls, reporting IGFBP-2 and IGFBP-3 at approximately 85 ng/mL and 91 ng/mL, respectively.[15] Although our findings have no impact on the IGFBP-2 estimates, the IGFBP-3 assays may be problematic and should be interpreted with caution until the issue of fragment immunoreactivity is revisited experimentally.

Another study with similar observations but different and mechanistically important conclusions was that of Schoen et al.,[29] who reported the presence of an IGFBP-3–specific protease in normal vitreous that is responsible for cleaving intact 46-kDa binding protein to an approximately 30-kDa form that was "undetectable by Western ligand blot analysis." Our studies revealed that normal vitreous is incapable of degrading intact IGFBP-3. The differences in our conclusions appear to be related to the experimental approach because their assay system combined vitreous with small amounts of serum as a source of intact IGFBP-3. We were able to duplicate their primary observation and demonstrated that both serum and vitreous are necessary for rapid IGFBP-3 cleavage. It is reasonably certain that their conclusions were based on a synergistic process involving enzymes or other factors from both sources. We also consistently demonstrated IGFBP-3 fragment detection by ligand blot analysis and bound the fragment to an IGF-II affinity column during purification, leading us to conclude that

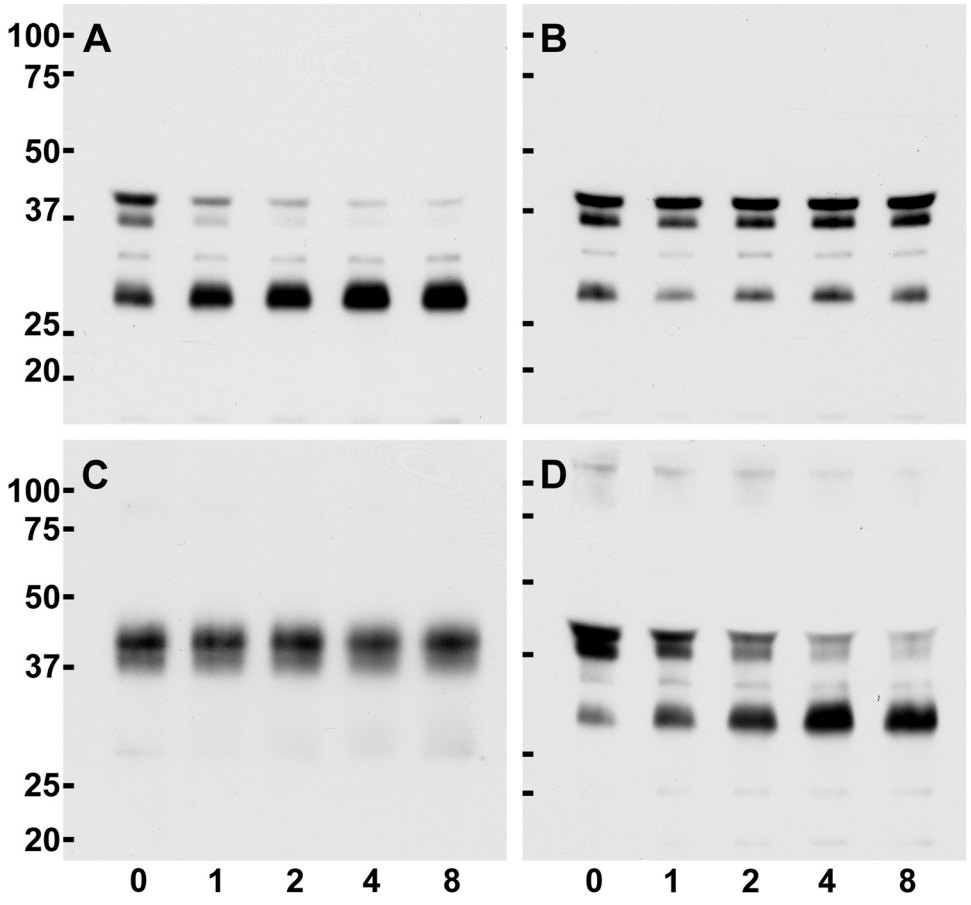

FIGURE 7. Samples of normal human plasma plus normal human vitreous (**A**), plasma alone (**B**), vitreous plus recombinant IGFBP-3 (**C**), or vitreous plus plasma plus recombinant IGFBP-3 (**D**) were incubated at 37°C for the indicated number of hours and then probed in Western ligand blots. Positions of molecular weight standards are indicated at the *left* of the figure.

the fragment retains ligand affinity. It is our speculation that the ligand blots performed in the Schoen et al.[29] study focused mainly on loss of the 46-kDa protein and that they were less sensitive to changes in the abundance of the ~29-kDa species. As a result, increases in the IGFBP-3 fragment resulting from proteolytic cleavage of the intact protein went undetected.

Finally, and most intriguing, are the functional implications raised by the absence of an active IGFBP-3 protease in normal vitreous. Where does the vitreous IGFBP-3 fragment come from and, if not generated locally, how does it get there? Our observations led us to speculate that the vitreous IGFBP-3 fragment originates in plasma and crosses the blood-vitreous barrier in much the same manner as other plasma proteins, such as albumin. Interestingly, the normal mechanism through which plasma proteins gain access to vitreous are still poorly understood, which is surprising considering that changes in this system may play major roles in the progression of several vitreoretinal pathologies involving changes in the IGF system. These observations should provide the necessary impetus for studies on blood vitreous barrier mechanism and functional characteristics.

Acknowledgments

The authors thank Christine Curcio, Lan Wang, and Martin Rudolf for their assistance obtaining the human vitreous specimens used in this study.

References

1. Frank RN. Diabetic retinopathy. *N Engl J Med.* 2004;350(1):48–58.
2. Guidry C. The role of Muller cells in fibrocontractive retinal disorders. *Prog Retin Eye Res.* 2005;24(1):75–86.
3. Sramek SJ, Wallow IH, Stevens TS, et al. Immunostaining of preretinal membranes for actin, fibronectin, and glial fibrillary acidic protein. *Ophthalmology.* 1989;96(6):835–841.
4. Weller M, Esser P, Heimann K, et al. [Idiopathic proliferative vitreoretinopathy: activation of microglial cells as the deciding factor]. *Ophthalmologe.* 1992;89(5):387–390.
5. Esser P, Heimann K, Wiedemann P. Macrophages in proliferative vitreoretinopathy and proliferative diabetic retinopathy: differentiation of subpopulations. *Br J Ophthalmol.* 1993;77(11):731–733.
6. Hosoda Y, Okada M, Matsumura M, et al. Epiretinal membrane of proliferative diabetic retinopathy: an immunohistochemical study. *Ophthal Res.* 1993;25(5):289–294.
7. Hiscott P, Gray R, Grierson I, et al. Cytokeratin-containing cells in proliferative diabetic retinopathy membranes. *Br J Ophthalmol.* 1994;78(3):219–222.
8. Mizutani M, Gerhardinger C, Lorenzi M. Muller cell changes in human diabetic retinopathy. *Diabetes.* 1998;47(3):445–449.
9. Guidry C, King JL, Mason JO 3rd. Fibrocontractive Muller cell phenotypes in proliferative diabetic retinopathy. *Invest Ophthalmol Vis Sci.* 2009;50(4):1929–1939.
10. Guidry C. Isolation and characterization of porcine Muller cells: myofibroblastic dedifferentiation in culture. *Invest Ophthalmol Vis Sci.* 1996;37(5):740–52.
11. Guidry C. Tractional force generation by porcine Muller cells: development and differential stimulation by growth factors. *Invest Ophthalmol Vis Sci.* 1997;38(2):456–468.
12. Guidry C, Bradley KM, King JL. Tractional force generation by human Muller cells: growth factor responsiveness and integrin receptor involvement. *Invest Ophthalmol Vis Sci.* 2003;44(3):1355–1363.
13. Guidry C, Feist R, Morris R, et al. Changes in IGF activities in human diabetic vitreous. *Diabetes.* 2004;53(9):2428–2435.
14. Grant M, Russel B, Fitzgerald C, et al. Insulinlike growth factors in vitreous: studies in control and diabetic subjects with neovascularization. *Diabetes.* 1986;35:416–420.
15. Meyer-Schwickerath R, Pfeiffer A, Blum WF, et al. Vitreous levels of the insulinlike growth factors I and II, and the insulinlike growth factor binding proteins 2 and 3, increase in neovascular eye disease: studies in nondiabetic and diabetic subjects. *J Clin Invest.* 1993;92(6):2620–2625.
16. Boulton M, Gregor Z, McLeod D, et al. Intravitreal growth factors in proliferative diabetic retinopathy: correlation with neovascular activity and glycaemic management. *Br J Ophthalmology.* 1997;81(3):228–233.
17. Burgos R, Mateo C, Canton A, et al. Vitreous levels of IGF-I, IGF binding protein 1, and IGF binding protein 3 in proliferative diabetic retinopathy: a case-control study. *Diabetes Care.* 2000;23(1):80–83.
18. Spranger J, Buhnen J, Jansen V, et al. Systemic levels contribute significantly to increased intraocular IGF- I, IGF-II and IGF-BP3 [correction of IFG-BP3] in proliferative diabetic retinopathy. *Horm Metab Res.* 2000;32(5):196–200.
19. Inokuchi N, Ikeda T, Imamura Y, et al. Vitreous levels of insulinlike growth factor-I in patients with proliferative diabetic retinopathy. *Curr Eye Res.* 2001;23(5):368–371.
20. Spranger J, Mohlig M, Osterhoff M, et al. Retinal photocoagulation does not influence intraocular levels of IGF- I, IGF-II and IGF-BP3 in proliferative diabetic retinopathy-evidence for combined treatment of PDR with somatostatin analogues and retinal photocoagulation? *Horm Metab Res.* 2001;33(5):312–316.
21. Hardwick C, Feist R, Morris R, et al. Tractional force generation by porcine Muller cells: stimulation by growth factors in human vitreous. *Invest Ophthalmol Vis Sci.* 1997;38(10):2053–2063.
22. Conover CA. Regulation and physiological role of insulinlike growth factor binding proteins. *Endocrine J.* 1996;43:p. S43–S48.
23. Clemmons DR. Role of insulinlike growth factor binding proteins in controlling IGF actions. *Mol Cell Endocrinol.* 1998;140(1–2):19–24.
24. Ferry RJ, Katz LEL, Grimberg A, et al. Cellular actions of insulinlike growth factor binding proteins. *Horm Metab Res.* 1998;31:192–202.
25. Baxter RC. Insulinlike growth factor (IGF)-binding proteins: interactions with IGFs and intrinsic bioactivities. *Am J Physiol Endocrinol Metab.* 2000;278(6):E967–E976.
26. Firth SM, Baxter RC. Cellular actions of the insulinlike growth factor binding proteins. *Endocr Rev.* 2002;23(6):824–854.
27. Duan C, Xu Q. Roles of insulinlike growth factor (IGF) binding proteins in regulating IGF actions. *Gen Comp Endocrinol.* 2005;142(1–2):44–52.
28. King JL, Guidry C. Insulinlike growth factor binding proteins modulate Muller cell responses to insulinlike growth factors. *Invest Ophthalmol Vis Sci.* 2004;45(12):4535–4542.
29. Schoen TJ, Waldbillig RJ, Searcy G, et al. Identification and partial characterization of a proteinase specific for insulinlike growth factor binding protein-3 in aqueous and vitreous humors. *Curr Eye Res.* 1995;14(2):127–135.
30. King JL, Guidry C. Muller cell production of insulinlike growth factor binding proteins in vitro: modulation with phenotype and growth factor stimulation. *Invest Ophthalmol Vis Sci.* 2004;45(12):4535–4542.
31. Laemmli U. Cleavage of structural proteins during the assembly of the head of bacteriophage T4. *Nature.* 1970;74:856–875.
32. Firth SM, Baxter RC. Characterisation of recombinant glycosylation variants of insulinlike growth factor binding protein-3. *J Endocrinol.* 1999;160(3):379–387.
33. Ahlsen M, Carlsson-Skwirut C, Jonsson AP, et al. A 30-kDa fragment of insulinlike growth factor (IGF) binding protein-3 in human pregnancy serum with strongly reduced IGF-I binding. *Cell Mol Life Sci.* 2007;64(14):1870–1880.
34. Yan X, Payet LD, Baxter RC, et al. Activity of human pregnancy insulinlike growth factor binding protein-3: determination by reconstituting recombinant complexes. *Endocrinology.* 2009;150(11):4968–4976.